Optik 126 (2015) 4087–4092

Contents lists available at ScienceDirect

Optik

journal homepage: www.elsevier.de/ijleo

Smear analysis for multi phase TDI CCD in panoramic remote sensing systems

Shuai Ding [a,b,*], Dejiang Wang [b], Haipeng Kuang [b], Yalin Ding [b]

[a] University of Chinese Academy of Sciences, Beijing 100084, China
[b] Key Laboratory of Airborne Optical Imaging and Measurement, Changchun Institute of Optics, Fine Mechanics and Physics, Chinese Academy of Sciences, Changchun 130033, Jilin, China

ARTICLE INFO

Article history:
Received 15 July 2014
Accepted 3 August 2015

Keywords:
TDI CCD
Clocking smear
Mismatch smear
Image quality
Modulation transfer function

ABSTRACT

Multi-phase Time Delay and Integration (TDI) remote sensing systems have the potential to introduce large amount of smear. Image resolution in the scan direction is usually lower than that in the cross scan direction. In designing these systems, it is helpful to understand how smear in the scan direction degrades the image quality. This paper presents a thorough understanding of the causes of along scan smear and a mathematical model that describes the smear in the along scan direction. Also the Modulation Transfer Function (MTF) losses are analyzed based on the novel model. At last a series of image simulations are performed in which along scan smear (with stage number N equal to 16, 32 and 96) is introduced.

1. Introduction

CCD (Charge Coupled Devices) detectors that works in TDI (Time Delay and Integration) mode has been widely employed in high-resolution remote sensing imaging systems. TDI CCD array takes multiple exposures of the same area and adds them automatically in the charge well. Thus it offers noise reduction and sensitivity accession without sacrificing spatial resolution [1–3]. However, any scanning imaging system will exhibit image smear which is caused by several reasons such as charge clocking, mismatch between the scan rate and the line rate, optical distortion, the terrain condition and [4] platform motion (pitch, roll, yaw) and speed. Usually the smear error in the along scan direction is larger than that in the cross scan direction [5,6].

Various models of along-scan smear have been introduced in the previous studies. Smith [4] suggested that $1/\Phi$ pixel smear occurs due to the charge transfer within each clock cycle, where Φ is the number of phases for each TDI stage. Also there is a displacement Δx for the mismatch between the image velocity on the focal plane and the clock cycle of the detector. Ma [7] claimed that one pixel smear due to mismatch for each TDI stage is introduced in the along scan direction. Wang [5] proposed that only $1/2\Phi$ pixel smear occurs within the imaging operation of a single TDI stage. Nonetheless, Smith simply assumed that the interval between different charge transfer steps is a fixed value and the mismatch smear Δx is a constant from one clock cycle to the next. Ma did not take the clocking smear into consideration. Besides, Wang did not mention the smear due to mismatch.

The purpose of this paper is to come up with a novel model of along-scan smear for a panoramic TDI CCD remote sensing system, and to discuss how it affects the MTF (Modulation Transfer Function) of the TDI CCD detector. In this paper, first we investigate the causes of the two main smear (clocking smear and mismatch smear) in the along scan direction. A mathematical model of along-scan smear for TDI CCD remote sensing system is established. Then, we deduce the MTF formula of the detector. The simulations of MTF curve have been done. Also we evaluate the image quality under different conditions. Conclusion is mentioned in the last section.

2. Image smear in the along scan direction

Image smear occurs when the scene moves across the detector while signal is integrated [8–10]. The analysis presented here is based on a panoramic TDI CCD remote sensing system. Fig. 1 illustrates the imaging principles of a typical panoramic aerial camera that uses TDI CCD. The imaging system scans the ground along the TDI CCD integration direction. The scanning mirror rotates along the flight direction which is perpendicular to the scan direction. Light beam from ground objects is reflected into the lens by the

* Corresponding author at: Chinese Academy of Sciences, Key Laboratory of Airborne Optical Imaging and Measurement, Changchun Institute of Optics, Fine Mechanics and Physics, Changchun 130033, Jilin, China. Tel.: +86 431 86708040/+86 431 86708617;
fax: +86 431 86708040/+86 431 85680049.
E-mail address: shuai.ding880413@gmail.com (S. Ding).

http://dx.doi.org/10.1016/j.ijleo.2015.08.012
0030-4026/

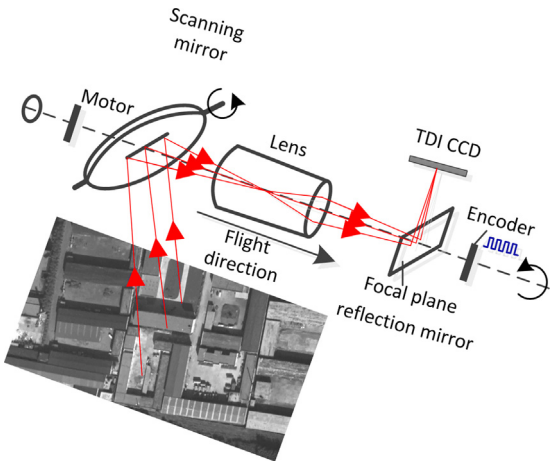

Fig. 1. Panoramic aerial camera imaging principles.

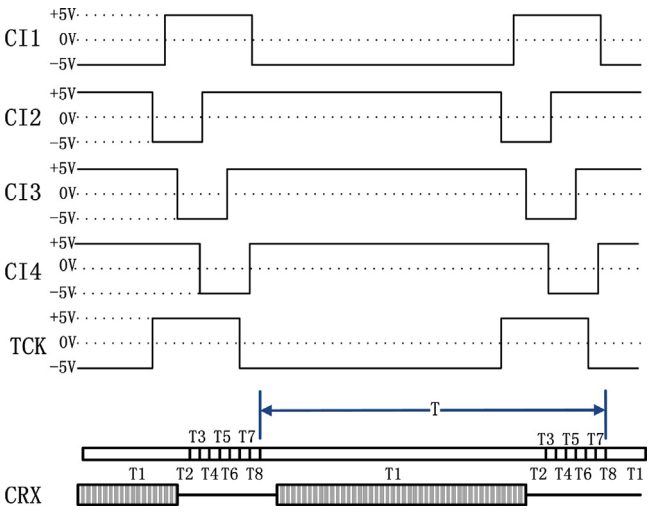

Fig. 3. Voltage levels for a 4-phase device.

scanning mirror firstly, then converged on the focal plane reflection mirror, and reflected onto the TDI CCD image plane at last [11]. The panoramic camera increases the ground area coverage by rolling the camera housing in the cross flight direction, and the rolling process is controlled by the encoder attached to it. As the image is swept across the array, the charge packets are clocked at the same rate [2]. A relative motion between the image and the target can be achieved in different ways. Here we discuss the two kinds of main smear in the along scan direction, which are the clocking smear and the mismatch smear.

2.1. Modeling of clocking smear

Clocking smear is the intrinsic nature of a remote sensing imaging system that uses a line scan CCD detector which cannot be eliminated by any kind of conventional image motion compensation methods. The platform of the imaging system moves and scans the ground continuously, while charge packet is clocked out discretely during each TDI stage. As a result, a relative motion between the image and the target ground scene occurs within each TDI stage.

Fig. 2 shows the structure of a four-phase TDI CCD [12]. There are mainly three functional regions comprising the TDI CCD: imaging area, isolation rows and horizontal readout register. The imaging area and isolation rows are controlled by the four-phase timing clock (CI1, CI2, CI3 and CI4). The charge is transferred line by line to the adjacent isolation rows for readout. The readout control is performed by CRX which is also a four-phase timing clock signal [13]. A four-phase system usually requires eight steps to transfer a charge packet from one pixel to the next. The charge is clocked out by pixel from the horizontal register. The charge transfer from one isolation row to another has to be stopped until all the charge in the horizontal register is clocked out. As a result, the readout process from horizontal shift register usually consumes more than 60% time of the whole charge transfer cycle. The model present here assumes T_1 takes up 65% time of the cycle and the other step equilibrates the time left as shown in Fig. 3.

Both the velocity and the displacement difference between the imaging pixel and the image point for a four-phase system are illustrated in Fig. 4, where the dash line represents the image point while the full line represents photosensitive pixel. Fig. 4 is

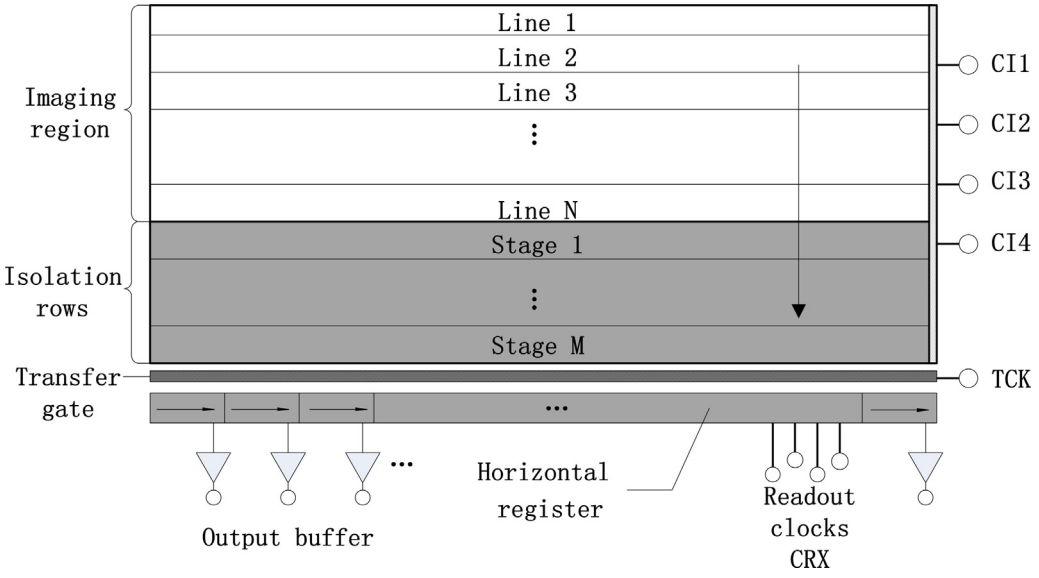

Fig. 2. TDI CCD structure.

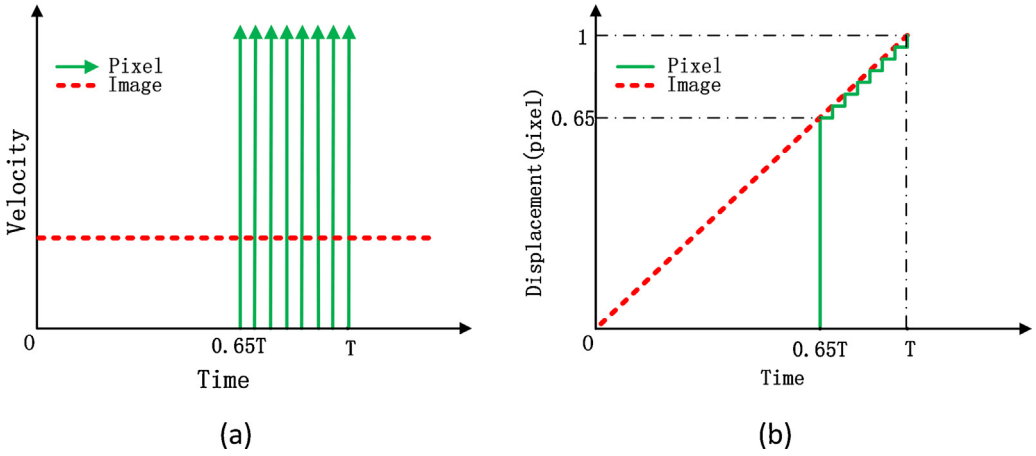

Fig. 4. Comparison between photosensitive pixel and image point within one transfer cycle. (a) Velocity comparison. (b) Displacement comparison.

corresponding to the model we proposed here that T_1 takes up 65% time of the whole cycle. The discrete transfer mode of charge packets leads to the relative motion between the image point (full line) and the pixel (dash line) shown in Fig. 4(b) which has been defined as clocking smear.

2.2. Modeling of mismatch smear

The scan rate needs to match with the line rate for a TDI CCD camera to function well [14,15]. Any asynchronization will result in the degradation of image quality [16]. Posture variation of the vehicle, change of temperature, defocus of optical system and jitter all affect the synchronization between the charge transfer rate and the image velocity on the focal plane. When mismatch smear occurs, the same target area will not be imaged by the same TDI stage precisely. The smear amount is usually proportional to the number of TDI stages. Though the smear amount is small within each integration cycle, with the increase of focal length and stages the mismatch smear increases significantly. Fig. 5 shows how the point source is imaged when there is no smear [Fig. 5(a)] and 1/2 pixel smear in the along scan direction [Fig. 5(b)]. We can see that the same target spot is not imaged by all N TDIs for the case shown in Fig. 5(b).

It is simply assumed that the amount of smear caused by mismatch between the scan rate and the line rate is a constant during each step of charge transfer in the previous studies [4,7]. However, the amount of the smear caused by many different reasons is not fixed during each integration step. It is modeled as a group of random values attributable to a certain distribution other than a fixed value. It is supposed that the displacement Δx obeys the zero-mean distribution. Though it is infeasible to apply a deterministic algorithm to the MTF, it does not mean that the MTF is not able to be figured out. Here we use Monte Carlo Method (MCM) to analyze how the mismatch smear influences the Modulation Transfer Function (MTF) of the TDI CCD.

3. MTF analyses

For a Φ-phase TDI CCD, we assume that the along scan direction is in the x direction, and the cross scan direction that is also the flight direction is in the y direction. The image with clocking smear can be modeled by convolving a blur function with the original smear free image:

$$I'(x,y) = I(x,y) \times \frac{E}{l}\mathrm{rect}\left(\frac{x}{l}\right), \tag{1}$$

where $I'(x,y)$ is the image with clocking smear, $I(x,y)$ is the image without smear, $\left(E/l\right)$ rect $\left(x/l\right)$ (see Fig. 6) is a rect function with width l which represents the amount of relative motion in the along scan direction, and E is the exposure intensity.

During the first time period of a charge transfer cycle, the displacement amount between the image point and the TDI CCD l_1 and the equivalent exposure intensity E_1 can be written as

$$l_1 = \frac{T_1}{T} \times p, \tag{2}$$

$$E_1 = \frac{T_1}{T}, \tag{3}$$

where T_1 represents the first clock cycle as shown in Fig. 3, and T represents the time cycle of charge packets transfer from one pixel to the next, and p is the detector pitch.

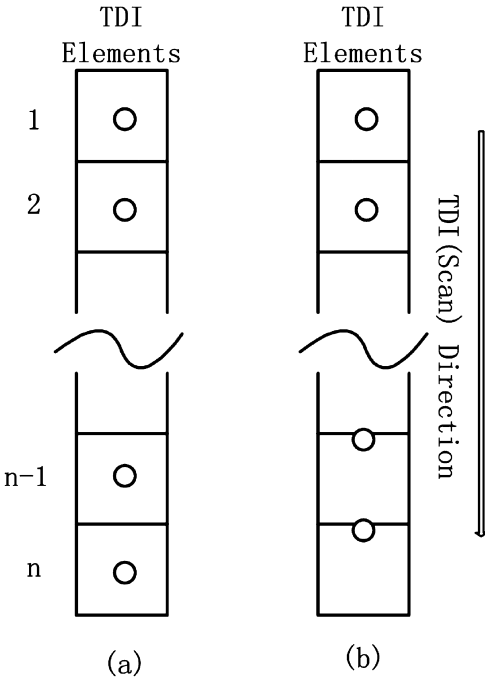

Fig. 5. Imaging system with no smear (a) and along scan smear (b).

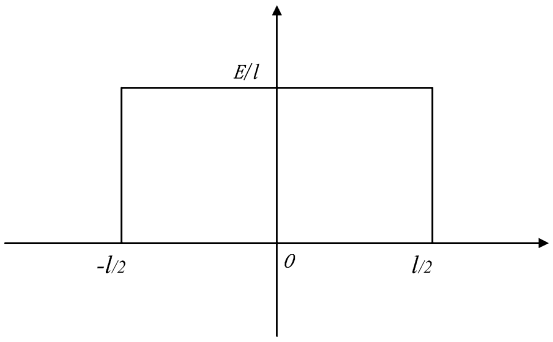

Fig. 6. Rect function used as the blur function.

We can get the blurred image after T_1 by substituting the l and E in Eq. (1) with Eqs. (2) and (3):

$$I_1'(x,y) = I(x,y) \times \frac{E_1}{l_1}\mathrm{rect}\left(\frac{x}{l_1}\right) = I(x,y) \times \frac{1}{p}\mathrm{rect}\left(\frac{x}{l_1}\right). \tag{4}$$

The image point on the focal plane has already moved l_1 before T_2, while the amount of charge packet movement is $p/2\Phi$. Thus the image can be written as $I\left(x - l_1 + \left(p/2\Phi\right), y\right)$ before T_2. Within the second clock cycle the displacement is $l_2 = \left(T_2/T\right) \times p$, the corresponding exposure intensity is $E_2 = T_2/T$. The image becomes:

$$I_2'(x,y) = I\left(x - l_1 + \frac{p}{2\Phi}, y\right) \times \frac{1}{p}\mathrm{rect}\left(\frac{x}{l_2}\right), \tag{5}$$

likewise, the blurred image after n clock cycle can be expressed as

$$I_n'(x,y) = I\left(x - \sum_{i=1}^{n} l_i + \frac{(n-1)p}{2\Phi}, y\right) \times \frac{1}{p}\mathrm{rect}\left(\frac{x}{l_n}\right), \tag{6}$$

where $n \le 2\Phi$ the final image after n steps of charge transfer can be derived by adding all the blurred images obtained from each step:

$$I'(x,y) = \sum_{i=1}^{2\Phi} I_i(x,y) =$$

$$\frac{1}{p}\left[\begin{array}{c} I(x,y) \times \mathrm{rect}\left(\frac{x}{l_1}\right) + I\left(x - l_1 + \frac{p}{2\Phi}, y\right) \times \mathrm{rect}\left(\frac{x}{l_2}\right) + \ldots \\ + I\left(x - \sum_{i=1}^{2\Phi} l_i + \frac{(n-1)p}{2\Phi}, y\right) \times \mathrm{rect}\left(\frac{x}{l_{2\Phi}}\right) \end{array}\right]. \tag{7}$$

Taking the Fourier transform yields:

$$I'(f_x, f_y) = \frac{I(f_x, f_y)}{p} \times \left[\begin{array}{c} l_1 \times \mathrm{sinc}(\pi l_1 f_x) + l_2 \times \mathrm{sinc}(\pi l_2 f_x) e^{-j2\pi\left(l_1 - p/2\Phi\right)f_x} + \ldots \\ + l_{2\Phi} \times \mathrm{sinc}(\pi l_{2\Phi} f_x) e^{-j2\pi\left(\sum_{i=1}^{2\Phi-1} l_i - \left((2\Phi-1)p/2\Phi\right)\right)f_x} \end{array}\right]. \tag{8}$$

The MTF due to clocking smear is defined as

$$\begin{aligned} \mathrm{MTF} = \frac{I'(f_x,f_y)}{I(f_x,f_y)} &= \frac{1}{p} \times \left[\begin{array}{c} l_1 \times \mathrm{sinc}(\pi l_1 f_x) + l_2 \times \mathrm{sinc}(\pi l_2 f_x) e^{-j2\pi\left(l_1 - (p/2\Phi)\right)f_x} + \ldots \\ + l_{2\Phi} \times \mathrm{sinc}(\pi l_{2\Phi} f_x) e^{-j2\pi\left(\sum_{i=1}^{2\Phi-1} l_i - \left((2\Phi-1)p/2\Phi\right)\right)f_x} \end{array}\right] \\ &= \frac{1}{p} \times \sum_{i=1}^{2\Phi} \left(l_i \times \mathrm{sinc}(\pi l_i f_x) e^{-j2\pi\left(\sum_{j=1}^{i} l_j - \left((i-1)p/2\Phi\right)\right)f_x} \right). \end{aligned} \tag{9}$$

Typically, remote sensing cameras use either two-phase or four-phase detectors. The amount of displacement during each charge transfer step is calculated according to Eq. (2). The results are listed in Table 1.

The MTF of a two-phase or a four-phase TDI CCD can be obtained using Eq. (9) and the figures listed in Table 1. The plot of clocking smear MTF is shown in Fig. 7.

Table 1
Displacement within each charge transfer clock.

Displacement	Two-phase	Four-phase
l_1	$13p/20$	$13p/20$
l_2	$7p/60$	$1p/20$
l_3	$7p/60$	$1p/20$
l_4	$7p/60$	$1p/20$
l_5	×	$1p/20$
l_6	×	$1p/20$
l_7	×	$1p/20$
l_8	×	$1p/20$

Taking the mismatch smear into consideration as well, there is a Δx displacement each charge transfer step. Δx is a random number as discussed in Section 2. The image location is displaced by an amount Δx before each charge transfer clock cycle while the image velocity is not properly matched with the line rate. The asynchronization increases the smear of each image collected at each charge transfer clock cycle by Δx. Thus we can get the MTF by adding Δx_i to each l_i in Eq. (9):

$$\mathrm{MTF}(f_x) = \frac{1}{p} \times \sum_{i=1}^{2\Phi} \left((l_i + \Delta x_i) \times \mathrm{sinc}(\pi (l_i + \Delta x_i) f_x) e^{-j2\pi\left(\sum_{j=1}^{i} (l_j + \Delta x_j) - \left((i-1)p/2\Phi\right)\right)f_x} \right). \tag{10}$$

The MTF for the linear smear associated with a detector having N TDI stages can be written as

$$\mathrm{MTF}_{\mathrm{smear}}(f_x) = \frac{1}{p} \times \sum_{n=0}^{N-1} \sum_{i=1}^{2\Phi} \left(\begin{array}{c} (l_i + \Delta x_i) \times \mathrm{sinc}(\pi (l_i + \Delta x_i) f_x) \times \\ e^{-j2\pi n\left(\sum_{j=1}^{i} (l_j + \Delta x_j) - \left(\left((i-1)p/2\Phi\right)f_x\right)\right)} \end{array} \right). \tag{11}$$

The amount of mismatch smear caused by various reasons is random within each charge transfer clock cycle. Here we use Monte Carlo method to develop the model of Δx. The Δx obeys the zero-mean distribution, its distribution interval is [−0.15,0.15] in pixels. Appling the model of Δx and Eq. (11), we plot an along-scan smear MTF diagram (see Fig. 8), where the spatial frequency is normalized to cycles/pixel. Note that the MTF curves shown in Fig. 8 are for three different TDI stages which are 16, 32 and 96. It is noticed that as the stage number becomes greater, the imaging system tends to have lower MTFs since the smear is worse.

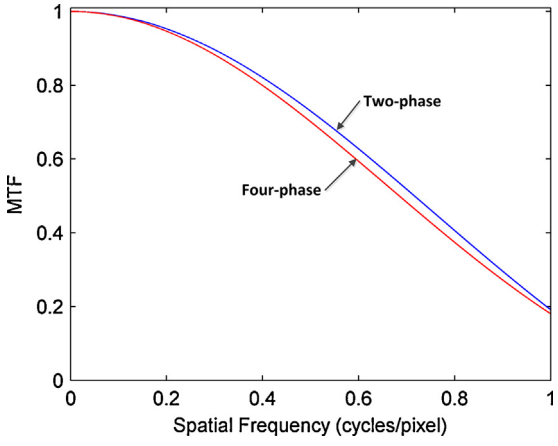

Fig. 7. Clocking smear MTF of a two-phase or a four-phase TDI CCD.

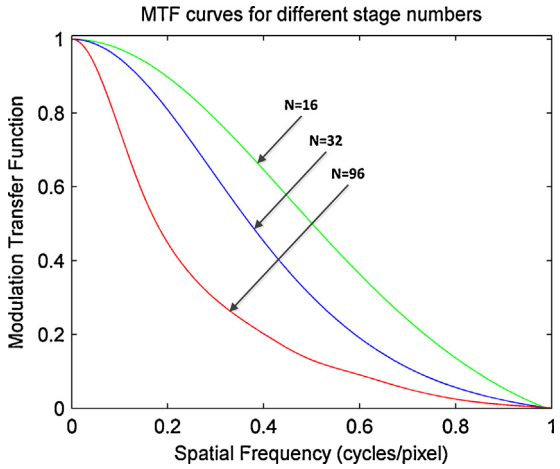

Fig. 8. MTF curves for different stage numbers.

Table 2
Imaging system characteristics.

Parameters	Value
Pixel	12 μm × 12 μm
Focal length	1000 mm
Relative aperture	1:6
Vehicle height	10 km
Detector phase number	4

4. Image simulations and evaluations

In order to understand the image quality of remote-sensing cameras with smear in the along-scan direction in terms of different TDI stages, images with along-scan smear of different TDI stages are simulated. The characteristics of imaging system used for simulation are summarized in Table 2. Scenes collected by this aerial camera were simulated with N equal to 16, 32 and 96. Fig. 9(a) to (d) shows a sample set of simulations for the same scene.

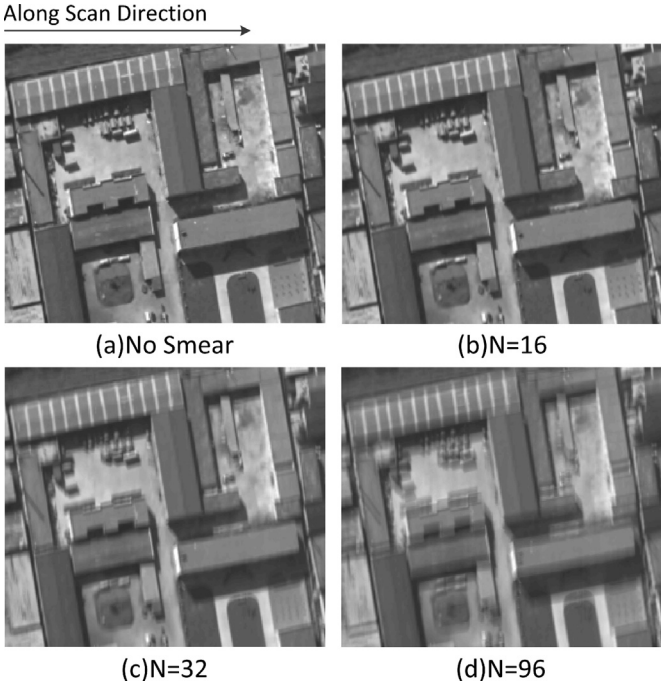

Fig. 9. Simulations of along scan smear in terms of different stages.

Fig. 9(a) shows the image with no along scan smear. Taking both the clocking and mismatch smear into consideration, the images become blurrier as illustrated in Fig. 9(b) to (d). The innate clocking smear of TDI CCD detectors degrades the image quality in the along scan direction. When it comes to the mismatch smear the images are simulated by using Monte Carlo Method as discussed earlier in the paper. Though the mismatch smear is not a certain value, the trend of the image quality is determined – the image does appear blurrier for higher stage number.

5. Conclusion

Image smear is always present in TDI CCD imaging systems. The clocking and mismatch smear in the along-scan direction leads to image quality degradation in that direction for a multi-phase TDI remote sensing system. Usually the clocking smear is neglected and the mismatch smear is considered simply as a fixed value. In this work, an elaborate mathematical model was established to describe the two main smear procedures in the along scan direction and analysis of the MTFs for imaging system with along scan smear of 16, 32, and 96 stages was considered. Also we used images collected by a certain aerial imaging system to simulate scenes with along-scan smear. It is found that with the TDI stages increasing, the image becomes blurrier.

Clocking smear is an intrinsic property of TDI CCDs which cannot be easily removed and mismatch smear is random values within each clock cycle for multi phase TDI imaging systems. However, the model developed in this paper assists remote sensing system designers to understand how the smear in the along scan direction affects the image quality.

Acknowledgements

This work is supported by the National Natural Science Foundation of China under Grant 61308099 and Grant 61304032.

References

[1] G.C. Holst, Electro-Optical Imaging System Performance, SPIE Optical Engineering Press, Bellingham, 2008.
[2] G.C. Holst, CCD Arrays Cameras and Displays, SPIE Optical Engineering Press, Bellingham, 1998.
[3] U. Bastian, M. Biermann, Astrometric meaning and interpretation of high-precision time delay integration CCD data, J. Astron. Astrophys. 438 (2005) 745–755.
[4] S.L. Smith, J. Mooney, T.A. Tantalo, R.D. Fiete, Understanding image quality losses due to smear in high-resolution remote sensing imaging systems, Opt. Eng. 38 (1995) 821–826.
[5] D.J. Wang, T. Zhang, H.P. Kuang, Clocking smear analysis and reduction for multi phase TDI CCD in remote sensing system, Opt. Express 19 (2011) 4868–4880.
[6] D.J. Wang, B. Dong, W.M. Li, C.Q. Jin, Influence of TDI CCD charge transfer on imaging quality in remote sensing system, Opt. Precis. Eng. 19 (2011) 2500–2506.
[7] T.B. Ma, Y.F. Guo, Y.F. Li, Precision of row frequency of scientific grade TDI CCD camera, Opt. Precis. Eng. 18 (2010) 2028–2035.
[8] Richard H. Vollmerhausen, Donald A. Reago Jr., Ronald G. Driggers, Analysis and Evaluation of Sampled Imaging Systems, SPIE Optical Engineering Press, Bellingham, 2010.
[9] G. Hochman, Y. Yitzhaky, N.S. Kopeika, Y. Lauber, M. Citroen, A. Stern, Restoration of images captured by a staggered time delay and integration camera in the presence of mechanical vibrations, Appl. Opt. 43 (2004) 4345–4354.
[10] U. Bastian, M. Biermann, Astrometric meaning and interpretation of high-precision time delay integration CCD data, Astron. Astrophys. 438 (2005) 745–755.

[11] Gang Li, Ping Jia, Method of improving the accuracy of image motion measurement for panoramic aerial cameras, Proc. SPIE. 7658 (2010) 76582A-1-5.
[12] G.C. Holst, CMOS/CCD Sensor and Camera System, SPIE Optical Engineering Press, Bellingham, WA, 2007.
[13] J.R. Janesick, Scientific Charge-Coupled Devices, SPIE Optical Engineering Press, Bellingham, WA, 2000.
[14] .R.D. Fiete, T. Tantalo, Image quality of increased along-scan sampling for remote sensing systems, Opt. Eng. 38 (1999) 815–820.
[15] R.D. Fiete, T. Tantalo, Comparison of SNR image quality metrics for remote sensing systems, Opt. Eng. 40 (2001) 574–585.
[16] J.L. Tong, M. Aydin, H.E. Bedell, Direction and extent of perceived motion smear during pursuit eye movement, Vis. Res. 47 (2007) 1011–1019.